

Effects of cold joint and loading conditions on chloride diffusion in concrete containing GGBFS

Yoo Sung-Won^a, Kwon Seung-Jun^{b,*}

^a Dept. of Civil Engineering, Woosuk University, Jeonbuk 565-701, South Korea

^b Department of Civil and Environmental Engineering, Hannam University, Daejeon 306-791, South Korea



HIGHLIGHTS

- Cold joint effect on chloride diffusion is investigated for normal concrete.
- GGBFS effect on chloride diffusion is also evaluated.
- Compressive and tensile stress effects on diffusion are quantitatively evaluated.
- The total effect of joint, GGBFS, and loading level is evaluated on diffusion.
- Diffusion increases linearly in cold joint concrete under compressive region.

ARTICLE INFO

Article history:

Received 28 October 2015

Received in revised form 31 March 2016

Accepted 2 April 2016

Available online 16 April 2016

Keywords:

Chloride diffusion

Cold joint

Loading conditions

GGBFS

ABSTRACT

RC (Reinforced Concrete) structures undergo deterioration and the initiated corrosion in the steel is considered as one of the most critical problems. For efficient construction of structures, construction joint should be installed, however cold joint occurs reluctantly due to delayed concrete placing and poor condition of the old concrete surface. The chloride ingress in cold joint concrete is more rapid than that in sound concrete, and it is also affected by loading conditions. This paper presents a quantitative evaluation on chloride diffusion coefficient considering the effects of cold joint and loading conditions. For the work, concrete samples with 0.6 of w/b (water to binder) ratio are prepared. Compressive and tensile stresses are induced with 30% and 60% of ultimate strength, respectively. The chloride diffusion coefficients in accelerated condition are measured under loading, and the effects of cold joint and loading levels are evaluated. In order to investigate an effect of GGBFS (Ground Granulated Blast Furnace Slag) on chloride diffusion, 40% of GGBFS replacement ratio is considered for OPC (Ordinary Portland Cement) and the GGBFS effect is evaluated considering cold joint and loading levels. The effects of stress level, pore structure improvement through GGBFS, and cold joint on chloride diffusion coefficient are quantitatively investigated.

© 2016 Elsevier Ltd. All rights reserved.

1. Introduction

Concrete is an attractive construction material and it has been widely utilized for its many advantages such as high durability, cost-benefit, and stable material supply [1]. Unlike structural steel, concrete contains pores, and the porosity and its connectivity play an important role in mass and ion transport. Pores in concrete are the main routes for ingress of chloride ion and the induced chloride ions usually cause a rapid corrosion initiation in the embedded

steel [2,3]. When corrosion starts, bond strength with concrete increases in the initial period, however it is rapidly reduced over 3–5% corrosion ratio due to rust around steel, micro cracks, and spalling of cover concrete [4,5]. RC (Reinforced Concrete) structures are always exposed to exterior loadings and the transport behavior of chloride ion is much affected by exterior stress level. Several researches investigate the effect of loading level on chloride diffusion, water permeation, and gas transport [6–8]. In the compressive region, mass/ion transport slightly decreases in the initial loading due to condensation of pores and interlocking of small particles. With increasing loading, their transport significantly increases due to development of micro cracks, and it still increases to the time when crack width is open to about 0.4 mm [9,10]. Recently the effect of crack on chloride diffusion has been

* Corresponding author.

E-mail addresses: imysw@woosuk.ac.kr (S.-W. Yoo), [\(S.-J. Kwon\).](mailto:jjuni98@hannam.ac.kr)

Table 1

Mix proportions for the tests.

Case	G _{max} (mm)	Slump (mm)	S/a (%)	w/b	Air content (%)	Unit weight: kg/m ³			
						W		S	
						Binder	C	Slag	
OPC	25	180	41.4	0.6	4.5	180	300	–	735
GGBFS						180	120		1040
									1020

w/b: Water to binder ratio, C: Cement, S: Sand, G: Coarse Aggregate.

Table 2

Chemical components of OPC and GGBFS.

Compositions	SiO ₂ (%)	Al ₂ O ₃ (%)	Fe ₂ O ₃ (%)	CaO (%)	MgO (%)	SO ₃ (%)	Ig. loss (%)	Physical properties	
								Specific gravity	Blaine (cm ² /g)
OPC	21.0	4.29	3.35	62.10	2.27	2.35	2.73	3.16	3214
GGBFS	29.98	14.55	0.50	45.92	4.90	1.84	0.2	2.89	4340

Table 3

Physical properties of sand and coarse aggregates.

Types	Items			
	G _{max} (mm)	Specific gravity (g/cm ³)	Absorption (%)	F.M.
Fine aggregate	–	2.60	1.00	2.70
Coarse aggregate	25	2.62	0.78	6.78

actively studied through analysis modeling and experimental work [9,11–14].

In concrete placing, construction joint should be installed for avoiding cracking but cold joint may occur due to delayed placing of ready-mixed concrete without surface treatment between old and new concrete, which causes not only reduction of shear strength but also reduction of corrosion resistance [15,16]. Ingress of harmful ions through cold joint section, which is similar as pre-damaged section, is reported to be more rapid than in sound concrete, so that many researches have been carried out focusing on carbonation, chloride attack, and water permeability in concrete containing cold joint [17,18], however they are mainly dependent on field investigation results. The severe deterioration can be found from field investigation but technique for evaluation of the chloride behavior considering stress conditions and mineral admixture effect is very limitedly studied.

2. Chloride diffusion in concrete with cold joint under loading

Previously explained, cold joint is half-discrete section due to delayed placing of ready-mixed concrete. The section between old and new concrete should be treated in a suitable manner like sand blasting and water jetting, however it is usually exposed to harsh environment. Concrete undergoes cracking in use and the cracks are the main route for additionally enlarged chloride ingress. In the previous models on chloride diffusion, capillary pores are usually considered as main routes [19,20]. When crack occurs, chloride diffusion coefficient increases to approximately 160 times for non-steady state condition based on accelerated diffusion test [9] and 5.5 times for steady state condition based on apparent diffusion test [12]. The changing increment depends on the core size since representative area contains both crack width and sound concrete area. The mass transport is also affected by loading types. In the compressive region, gas permeability slightly decreases to about 60% of peak load and significantly increases to failure status [21], which shows similar trend with water permeability [7]. It is reported that chloride diffusion has similar trend

as gas and water permeability, showing more rapid diffusion/-transportation under tensile stress than compressive stress [8,22–24]. Recently an analytical modeling on diffusion coefficient under loadings is proposed with porosity and volumetric strain [24]. Many researches with experimental and analytical work have been conducted on evaluating the relationships between loading level and changing diffusion and permeation, however the effect of cold joint and mineral admixture on their relationship has not been considered.

3. Experimental program

3.1. Concrete preparation with cold joint

Concrete samples with OPC (Ordinary Portland Cement) and 40% replacement of GGBFS are prepared. The water to binder ratio is fixed as 0.6. The mix proportions and chemical compositions for OPC and GGBFS are listed in Table 1 and Table 2. The physical properties of sand and coarse aggregate are listed in Table 3.

For the compressive and tensile strength test, cylindrical (diameter 100 mm × height 200 mm) and rectangular parallelepiped specimens (100 mm × 100 mm × 50 mm) are prepared, respectively. The tests for strength are performed at the age of 28 and 91 days for evaluation of long-term strength development. For inducing cold joint, concrete is placed to a half and exposed to room condition for 24 h. The rest is filled with the same mixture after 24 h and then exposed to the same condition for 24 h. After removal of cast, the concrete samples are kept in water-submerged condition to 91 days. The photos for concrete samples with cold joint are shown in Fig. 1. In order to evaluate the cold joint effect on chloride diffusion coefficient, the cold joint section is set without surface treatment.

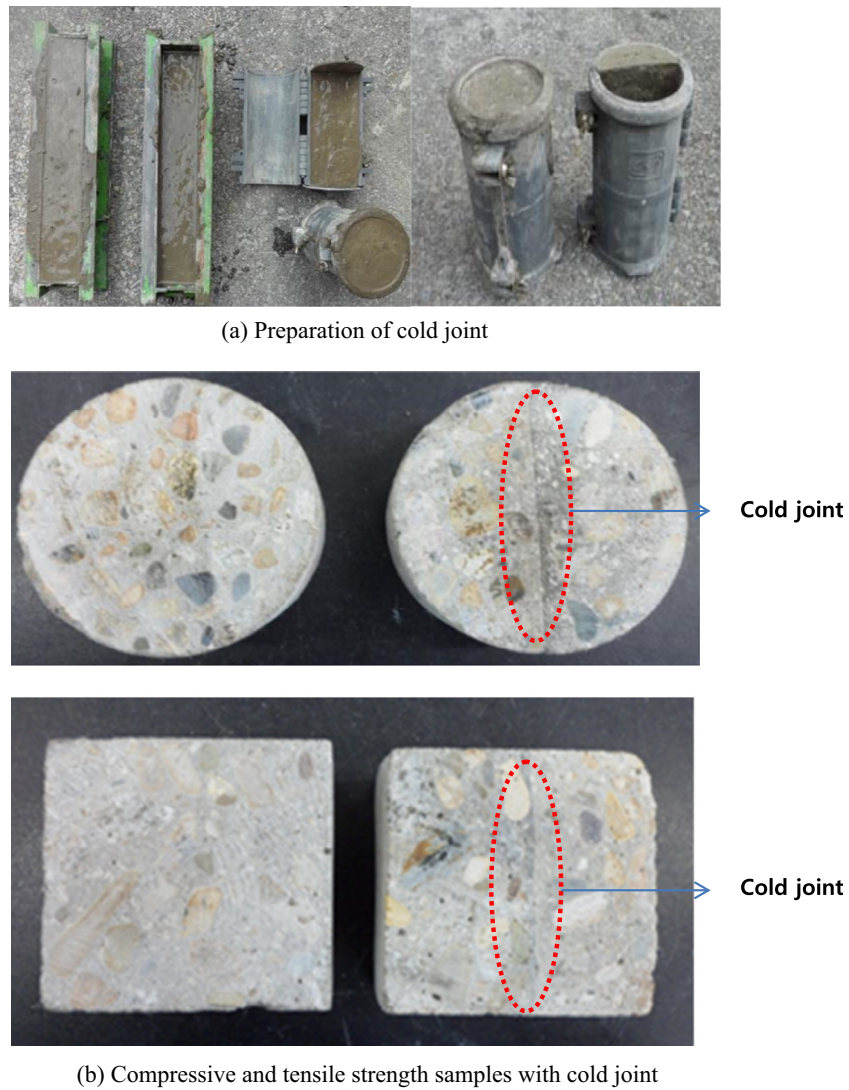
3.2. Chloride diffusion coefficient

For measuring chloride diffusion coefficient in concrete containing OPC and GGBFS, a diffusion cell is set up referred to ASTM C 1202 [25]. The calculation of the diffusion coefficient, so called non-steady state migration diffusion coefficient, is performed based on the Tang's method using silver nitrate solution (0.1 N, AgNO₃) as an indicator [26,27]. The diffusion coefficient in non-steady state conditions is calculated through Eq. (1).

$$D_{rcpt} = \frac{RTL}{zFU} \frac{x_d - \alpha\sqrt{x_d}}{t}, \quad \alpha = 2\sqrt{\frac{RTL}{zFU}} \text{erf}^{-1} \left[1 - \frac{2C_d}{C_0} \right] \quad (1)$$

where D_{rcpt} is diffusion coefficient in non-steady state condition (m²/s), R is universal gas constant (8.314 J/mol K), T is absolute temperature (K), L is thickness of specimen (m), z is ionic valence (=1.0), F is Faraday constant (=96,500 J/V mol), U is applied potential (V), t is test duration time (s), C_d is the chloride concentration at which the color changes when using a colorimetric method for measuring x_d based on the references [26,27]. C_0 is chloride concentration in the upstream solution (mol/l), erf^{-1} is the inverse of the error function. The conditions of accelerated diffusion test are listed in Table 4 and test setup for RCPT is shown in Fig. 2.

In order to prevent interference of edge effect, 10 mm of each side is ignored for calculation of chloride penetration depth.

**Fig. 1.** Concrete samples with cold joint.

3.3. Loading conditions

In order to induce compressive and tensile stress, each side of concrete is coated with epoxy except for front and back side, and steel frame is installed on the concrete samples. The effect of loading on chloride diffusion is reported to be non-linear so that two loading cases are considered. Ultimate loading is firstly evaluated for evaluation of strength, and then 30% and 60% of peak loads are induced for tensile and compressive stresses, respectively. When inducing the designated loading, the frames in top and bottom are fixed. Strain gauges are attached on the concrete surface and confining frame for monitoring the changes in strain. The intended load is slightly reduced due to slip of frame fixing, so that the final measured strength is considered as the loading level. Before RCPT (Rapid Chloride Penetration Test), the gauge on the concrete surface is removed and the strain of the reference gauge on the confining steel frame is monitored during the test for observing additional loss of stress due to frame relaxation. For compressive stress inducing, rectangular samples ($100 \times 100 \times 50$ mm) are used and cylindrical samples (100 mm diameter and 50 mm thickness) are also used for tensile stress as well. The samples may have micro cracks over 60% level of loading. This study assumes sound concrete and cold joint section, so that the crack effect on diffusion is merged in loading effect which can enlarge or reduce chloride diffusion coefficient. The test setup for inducing loads and fixed samples are shown in Fig. 3.

The strain variations during loading and the reference curve of stress-strain are shown in Fig. 4. In Fig. 4(a) and (b), the strain drop happens due to unloading and imperfect fixing, but they kept constant after fixing frame. In the reference curve in Fig. 4(c), the final stain level (300–400 stains) in Fig. 4(a) and (850–1000 stains) in Fig. 4(b) are assumed as 30% and 60% of loading ratio, respectively. As shown in Fig. 4(a) and (b), excess loading of 30% and 60% level can cause additional damage to concrete, however the effect of damage from overloading is assumed to be small.

Table 4
Diffusion cell and test conditions.

Conditions	Cathode	Anode	Applied voltage	Thickness	Applied Period
	0.5 M NaCl	0.3 M NaOH	30V	50 mm	6, 8 h

**Fig. 2.** Test setup for RCPT.

In tensile loading, the same procedures are repeated for cylindrical sample. The strains of reference gauge on the steel frame to loading direction are shown in Fig. 5, which shows almost constant for 6 hours of RCPT.

4. Evaluation of chloride diffusion coefficient considering effects of loading conditions, GGBFS, and cold joint

4.1. Test results

4.1.1. Compressive and tensile strength

Compressive strength for standard sample is measured at the age of 28 days and 91 days. The averages of the compressive strength are 26.8 MPa for OPC and 25.2 MPa for GGBFS concrete at the age of 28 days, however higher compressive strength is evaluated for GGBFS concrete with 33.1 MPa while OPC concrete shows 31.0 MPa at 91 days. The enhanced physical performance in GGBFS concrete can be explained by additionally produced CSH and reduced porosity due to latent hydration [1,28,29]. The results are shown in Fig. 6. The test results of the concrete sample for RCTP at the age of 91 days are listed in Table 5, which shows reasonable strength results for OPC and GGBFS concrete. The tensile strength is 12.0–12.3% level of compressive strength. Cold joint section is very vulnerable to direct tensile loading so that the cold joint sections (OJ-T and SJ-T) are subjected to load with angle difference by 30 degree, which shows 2.7 MPa of tensile strength (8.0–8.3% of the compressive strength).

4.1.2. Chloride diffusion coefficient

For the samples at the age 91 days, test results of chloride diffusion coefficient are shown in Fig. 7. Without loading and cold joint effect, GGBFS concrete shows the least diffusion coefficient of $6.6 \times 10^{-12} \text{ m}^2/\text{s}$, which shows 27.8% of result in OPC concrete. The excellent resistance to chloride penetration in GGBFS concrete can be found in many previous researches [1,2,27–29]. The effects of loading condition and cold joint on chloride diffusion coefficients are investigated in Section 4.2 in detail.

The photos after spraying AgNO₃ indicator are shown in Fig. 8, where increasing chloride penetration depths are well observed with loading ratios. The cracks inside concrete due to loadings are presented in Fig. 9.

4.2. Various effects of loading and cold joint on diffusion coefficient

Previously explained, the type and level of loading are the main parameters which can change the diffusion behavior in concrete since tensile strength of concrete is very small compared with compressive strength. Several researches shows that rapid mass transport is caused under tensile region due to micro cracking in the transit zone between aggregate and cement hydrates. In the compressive region, similar or reduced transport is observed to 40–50% of loading and then enlarged transport is reported afterwards due to micro cracking [6,7]. It is very interesting that con-



(a) Test setup for loading



(b) Samples for tensile stress



(c) Samples for compressive stress

Fig. 3. Test setup for load inducing.

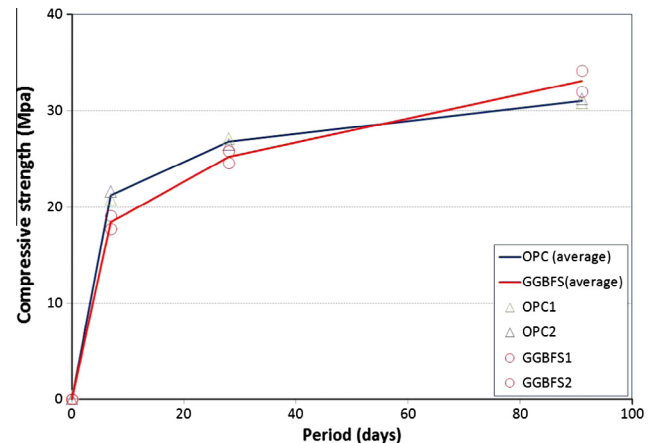
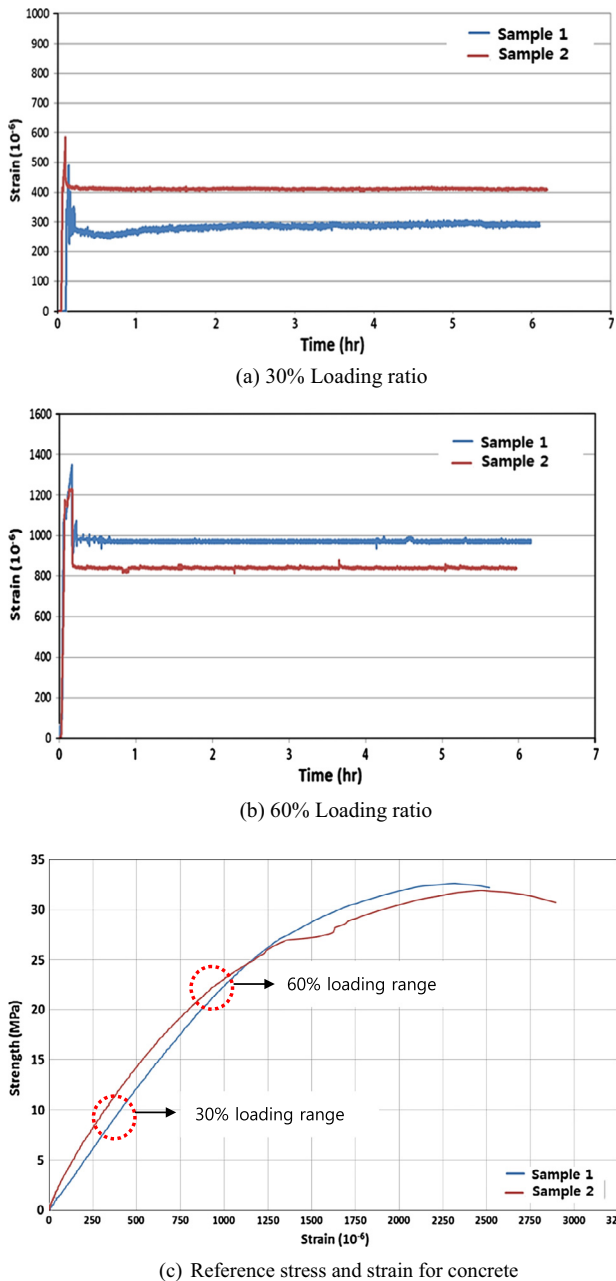


Fig. 6. Compressive strength at the age of 28 and 91 days (standard size).

Table 5
Compressive and tensile strength for RCPT samples (91 days).

Systems	Strength (MPa)				
	1	2	3	Average	
Compressive strength	O-C	32.6	31.8	32.5	32.3
	OJ-C	32.3	32.8	32.7	32.6
	S-C	33.9	34	34.4	34.1
	SJ-C	34.1	33	33.7	33.6
Tensile strength	O-T	3.7	4.1	3.9	3.9
	OJ-T	2.6	2.9	2.6	2.7
	S-T	4.2	4.2	4.2	4.2
	SJ-T	2.8	2.6	2.7	2.7

O: OPC, S: GGBFS, J: Cold joint C: Compressive stress, T: Tensile stress.

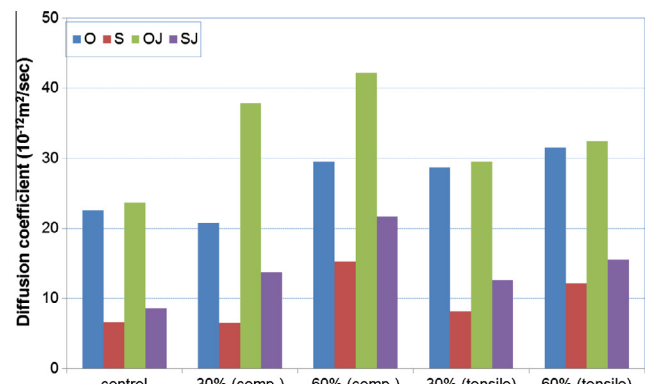


Fig. 7. Chloride diffusion coefficient considering cold joint, loading level, and GGBFS (averages).

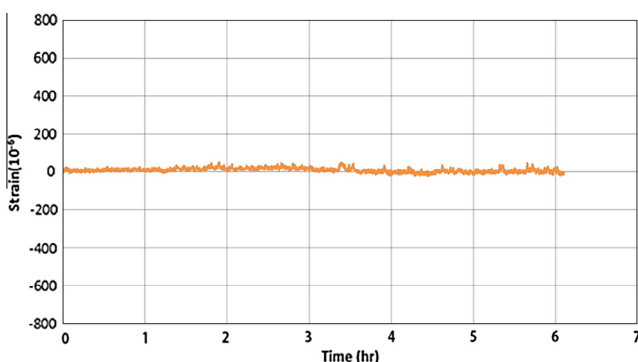


Fig. 5. Constant strain during RCPT (loading direction).

crete samples with cold joint show enlarged diffusion in spite of 30% of compressive loading, which accounts for the more permission of chloride ion in the small compressive stress. In the OPC concrete without cold joint, the enlarged diffusion is consistent with the previous results in compressive resign however the results in tensile region underestimate the diffusion coefficients by 20–30% compared with the previous research [30,31]. It is thought that the tensile loading level in the paper is slightly small for avoiding local failure of the samples. The chloride diffusion coefficients under compressive and tensile stress are shown in Fig. 10. In Table 6, test results and the ratios to control are listed. The results are replotted for normalized diffusion with varying stress level in Fig. 11 and the regression analysis results are summarized in Table 7 with determination coefficients.

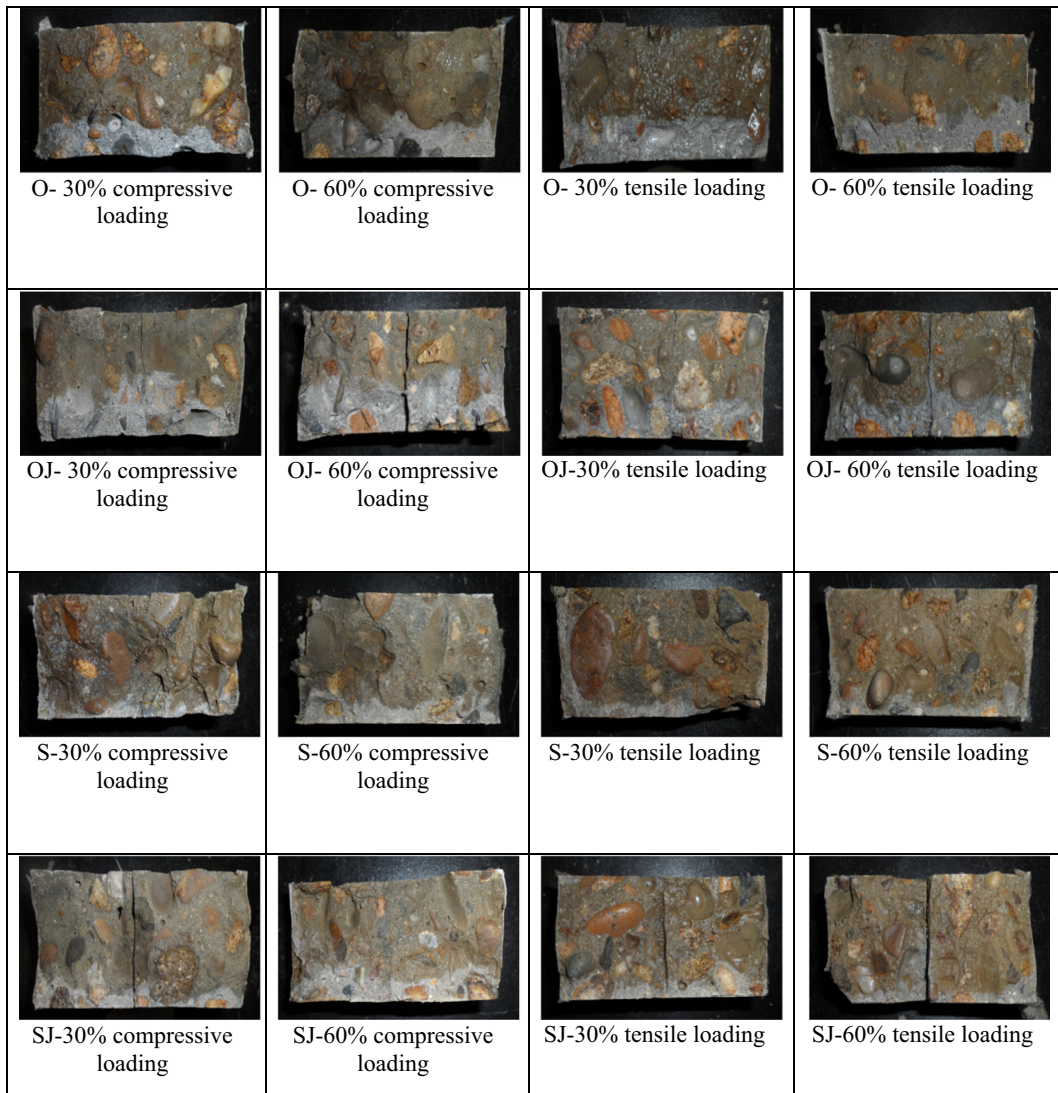


Fig. 8. Chloride penetration depth with increasing loading level.

From the above figures, OPC and GGBFS concrete are evaluated to contain slightly reduced diffusion coefficient to 30% of loading level, which are 0.94 times for OPC and 0.98 times for GGBFS in the compressive region. When loading increases to 60%, chloride diffusion coefficient increases to 1.34 times for OPC and 2.32 for GGBFS concrete. In tensile region, diffusion coefficients linearly increase 1.24–1.47 time to 30% of loading and 1.37–1.85 times to 60% of loading, respectively. The reason for more increasing ratio in GGBFS concrete is that the results without loading have small value compared with those in OPC concrete. The GGBFS concrete shows better resistance to chloride ingress than OPC concrete both for cold joint and loading cases. In the tensile region, cold joint effect is evaluated to be much lower than loading effect since the gradient is small regardless of joint (dot line in Fig. 11) with linear relation with loading level to 0.6 of peak load. The pattern in OPC concrete is consistent with that in GGBFS concrete as shown in Fig. 11(b).

The penetration depth in cold joint concrete with GGBFS shows very sharp intrusion and this means chloride intrusion perpendicular to migrating direction is very small while results in normal concrete contains smooth contour as shown in Fig. 12.

The effect of loading conditions on diffusion behavior is reasonably consistent with the previous researches and the enlarged

diffusion ratios are quantitatively evaluated for concrete with GGBFS and cold joint. However the ratios of diffusion coefficient may be changed in concrete with lower w/c ratio (high strength concrete) since diffusion coefficient in control case is very small. Furthermore effect of cold joint on diffusion can vary in wide range when surface treatment is not conducted. The work can be improved through consideration of treatment for cold joint surface, diffusion behavior in high strength concrete, and accurate loading level with perfect confining systems.

5. Conclusions

The conclusions on effects of cold joint and loading conditions on chloride diffusion in concrete containing GGBFS are as follows

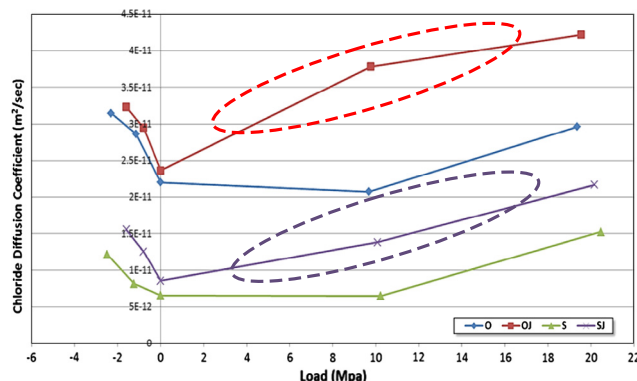
- Chloride diffusion coefficient is evaluated to decrease to 30% of loading level and increases afterwards in the compressive condition. When loading level increases to over 60%, diffusion coefficient increases to 1.34–1.78 times for normal concrete and 2.32–2.52 times for GGBFS concrete. In particular chloride diffusion coefficient goes up with quadratic shape for normal concrete, however linearly increasing shape is evaluated for cold joint concrete regardless of binder type.



(a) Cracks on surface (60% of tensile loading)



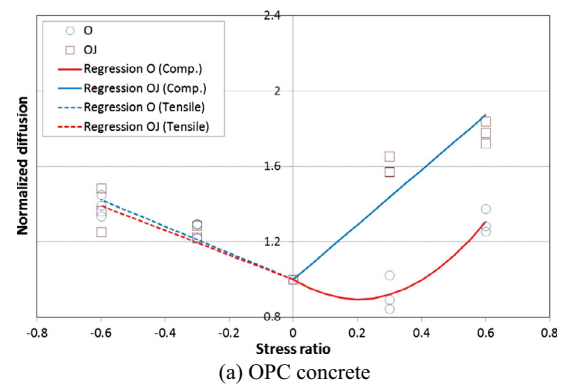
(b) Cracks on surface (60% of compressive loading)

Fig. 9. Cracks on loading conditions.**Fig. 10.** Chloride diffusion coefficients under compressive and tensile stress.**Table 6**

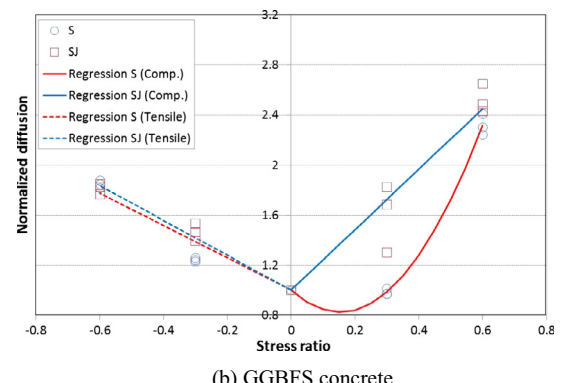
Chloride diffusion coefficient considering loading effects (averages).

	Load	Diffusion coefficient ($\times 10^{-12} \text{ m}^2/\text{s}$)		
		Control	30%	60%
Compressive loading	O	22.0 (1.00)	20.8 (0.94)	29.5 (1.34)
	S	6.6 (1.00)	6.5 (0.98)	15.3 (2.32)
	OJ	23.7 (1.00)	37.9 (1.6)	42.2 (1.78)
	SJ	8.6 (1.00)	13.8 (1.6)	21.7 (2.52)
Tensile loading	O	22.0 (1.00)	28.7 (1.30)	31.5 (1.43)
	S	6.6 (1.00)	8.2 (1.24)	12.2 (1.85)
	OJ	23.7 (1.00)	29.5 (1.24)	32.4 (1.37)
	SJ	8.6 (1.00)	12.6 (1.47)	15.6 (1.81)

O: OPC, S: GGBFS, OJ: OPC with cold joint, SJ: GGBFS with cold joint.



(a) OPC concrete



(b) GGBFS concrete

Fig. 11. Chloride diffusion coefficients under stress level.

Table 7

Regression results for normalized diffusion coefficient with loading levels.

Systems		Regression analysis	R ²
Compressive loading	O	2.582x ² – 1.040x + 1	0.90
	S	7.492x ² – 2.298x + 1	0.99
	OJ	1.455x + 1	0.71
	SJ	2.417x + 1	0.87
Tensile loading	O	0.705x + 1	0.82
	S	1.293x + 1	0.90
	OJ	0.653x + 1	0.71
	SJ	1.395x + 1	0.96

O: OPC, S: GGBFS, OJ: OPC with cold joint, SJ: GGBFS with cold joint.

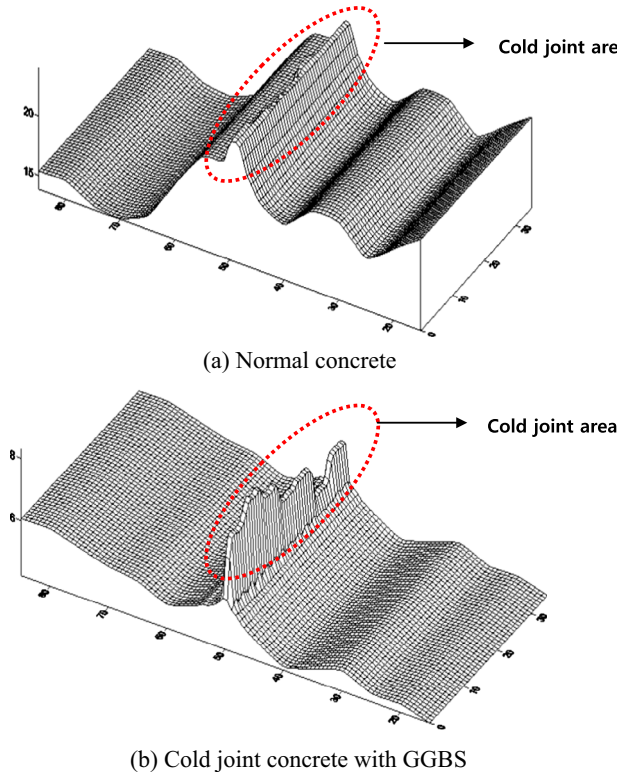


Fig. 12. Contour of chloride penetration depth in concrete with cold joint.

In the tensile condition, loading effect is much clear than cold joint effect on chloride diffusion. The results linearly increase to 60% of loading level. Concrete with cold joint increases to 1.37 times for OPC and 1.81 for GGBFS concrete but the value in cold joint concrete with GGBFS is only 48% level ($15.6 \times 10^{-12} \text{ m}^2/\text{s}$) of normal concrete with cold joint ($32.4 \times 10^{-12} \text{ m}^2/\text{s}$).

2) GGBFS is evaluated to be very effective for resisting chloride penetration and it still works for not only sound concrete but also cold joint concrete. Without loading, diffusion coefficient is reduced to 36% ($8.6 \times 10^{-12} \text{ m}^2/\text{s}$) through 40% replacement ratio of GGBFS. When compressive loading level reaches 60% for cold joint concrete, the result increases from $23.7 \times 10^{-12} \text{ m}^2/\text{s}$ to $42.2 \times 10^{-12} \text{ m}^2/\text{s}$ for OPC concrete while GGBFS concrete changes from $8.6 \times 10^{-12} \text{ m}^2/\text{s}$ and $21.7 \times 10^{-12} \text{ m}^2/\text{s}$. In the tensile condition with 60% loading level, they linearly increases to $32.4 \times 10^{-12} \text{ m}^2/\text{s}$ for OPC concrete and $15.6 \times 10^{-12} \text{ m}^2/\text{s}$ for GGBFS concrete, respectively, which shows the excellent resistance to chloride ingress.

Acknowledgement

This research was supported by Basic Science Research Program through the National Research Foundation of Korea (NRF) funded by the Ministry of Science, ICT & Future Planning (No. 2015R1A5A1037548). This was also supported by Basic Science Research Program through the National Research Foundation of Korea (NRF) funded by the Ministry of Education (NRF-2013R1A1A2060114).

References

- [1] P.K. Metha, P.J.M. Monteiro, *Concrete: Structure, Properties, and Materials*, Prentice-Hall Inc., Englewood Cliffs: New Jersey, 1993.
- [2] H.-W. Song, S.-W. Park, C.H. Lee, S.-J. Kwon, Service life prediction of concrete structures under marine environment considering coupled deterioration, *J. Restorat. Build. Monu.* 12 (2006) 265–284.
- [3] T. Ishida, K. Maekawa, Modeling of durability performance of cementitious materials and structures based on thermo-hygro physics, in: *Proc-PRO 29: Life Prediction and Aging Management of Concrete Structures*, vol. 1, RILEM, 2003, pp. 39–49.
- [4] L. Chung, J.J.H. Kim, S.T. Yi, Bond strength prediction for reinforced concrete members with highly corroded reinforcing bars, *Cem. Concr. Compos.* 30 (2008) 603–611.
- [5] L. Chung, H. Najm, P. Balaguru, Flexural behavior of concrete slabs with corroded bars, *Cem. Concr. Compos.* 30 (2008) 184–193.
- [6] M. Hoseini, V. Bindiganavile, N. Banthia, The effect of mechanical stress on permeability of concrete: a review, *Cem. Concr. Compos.* 31 (2009) 213–220.
- [7] N. Banthia, A. Biparva, S. Mindess, Permeability of concrete under stress, *Cem. Concr. Res.* 35 (2005) 1651–1655.
- [8] A. Kermani, Permeability of stressed concrete, *Build. Res. Inf.* 19 (1991) 360–366.
- [9] S.S. Park, S.-J. Kwon, S.H. Jung, Analysis technique for chloride penetration in cracked concrete using equivalent diffusion and permeation, *Constr. Build. Mater.* 29 (2012) 183–192.
- [10] S.S. Park, S.-J. Kwon, S.H. Jung, S.W. Lee, Modeling of water permeability in early aged concrete with cracks based on micro pore structure, *Constr. Build. Mater.* 27 (2012) 597–604.
- [11] A.M. Ghadehbari, S.P. Shah, A. Karr, Estimation of water flow through cracked concrete under load, *ACI Mater. J.* 97 (2000) 567–575.
- [12] S.-J. Kwon, U.-J. Na, S.S. Park, S.H. Jung, Service life prediction of concrete wharves with early-aged crack: probabilistic approach for chloride diffusion, *Struct. Saf.* 31 (2009) 75.
- [13] B. Gerard, J. Marchand, Influence of cracking on the diffusion properties of cement-based materials: part I: influence of continuous cracks on the steady state regime, *Cem. Concr. Res.* 30 (2000) 37.
- [14] N. Gowripalan, V. Sirivivatnanon, C.C. Lim, Chloride diffusivity of concrete cracked in flexure, *Cem. Concr. Res.* 30 (2000) 725.
- [15] JSCE, *Concrete Cold Joint Problems and Countermeasures*, Concrete Library Japan 387 Society of Civil Engineering, 2000, 103; [in Japanese].
- [16] ACI 224.3R-95, *Joints in Concrete Construction*, American Concrete Institute, USA, 2001, 389 Reapproved.
- [17] K. Yokozeki, K. Okada, T. Tsutsumi, K. Watanabe, Prediction of the service life of RC with crack exposed to chloride attack, *J. Sympos. Rehab. Concr. Struct.* 10 (1998) 1 [in Japanese].
- [18] S.-J. Kwon, U.-J. Na, Prediction of durability for RC columns with crack and joint under carbonation based on probabilistic approach, *Int. J. Concr. Struct. Mater.* 5 (2011) 11–18.
- [19] K. Maekawa, T. Ishida, T. Kishi, Multi-scale modeling of concrete performance, *J. Adv. Concr. Technol.* 1 (2003) 91–26.
- [20] M. Nagesh, B. Bishwajit, Modelling of chloride diffusion in concrete and determination of diffusion coefficients, *ACI Mater. J.* 95 (1998) 113.
- [21] M. Choinska, A. Khelidj, G. Chatzigeorgiou, G. Pijaudier-Cabot, Effects and interactions of temperature and stress-level related damage on permeability of concrete, *Cem. Concr. Res.* 37 (2007) 79–88.
- [22] A.D. Tegguer, S. Bonnet, A. Khelidj, V. Baroghel-Bouny, Effect of uniaxial compressive loading on gas permeability and chloride diffusion coefficient of concrete and their relationship, *Cem. Concr. Res.* 52 (2013) 131–139.
- [23] Y. Yang, H.Z. Tong, S.F. Xu, Effects of load level on water permeability of concrete, in: *The First International Conference on Micro-structure Related Durability of Cementitious Composites*, Nanjing, China, 2008, p. 545.
- [24] X. Du, L. Jin, R. Zhang, Chloride diffusivity in saturated cement paste subjected to external mechanical loadings, *Ocean Eng.* 95 (2015) 1–10.
- [25] ASTM C1202, Electrical indication of concrete's ability to resist chloride ion penetration, in: *Annual Book of American Society for Testing Materials Standards*, 1993.
- [26] N. Otsuki, S. Nagataki, K. Nakashita, Evaluation of AgNO₃ solution spray method for measurement of chloride penetration into hardened cementitious matrix materials, *ACI Mater. J.* 89 (1992) 587–592.
- [27] L. Tang, Electrically accelerated methods for determining chloride diffusivity in concrete-current development, *Mag. Concr. Res.* 48 (1996) 173–179.

- [28] H.-W. Song, S.-J. Kwon, Evaluation of chloride penetration in high performance concrete using neural network algorithm and micro pore structure, *Cem. Concr. Res.* 39 (2009) 814–824.
- [29] S.-H. Lee, S.-J. Kwon, Experimental study on the relationship between time-dependent chloride diffusion coefficient and compressive strength, *J. Korea Concr. Inst.* 24 (2012) 715–726 [in Korean].
- [30] Y.-W. Bae, N.-G. Lim, Resistance of chloride penetration of fiber reinforced concrete under loading conditions, *J. Korea Arch. Inst.* 28 (2012) 67–74 [in Korean].
- [31] D.-H. Kim, N.-G. Lim, T. Horiguchi, Effect of compressive loading on the chloride penetration of concrete mixed with granulated blast furnace slag, *J. Arch. Constr. Inst.* 9 (2009) 71–78 [in Korean].